Luminal and cytosolic pH feedback on proton pump activity and ATP affinity of V-type ATPase from Arabidopsis

Rienmüller, Florian ; Dreyer, Ingo ; Schönknecht, Gerald ; Schulz, Alexander ; Schumacher, Karin ; Nagy, Réka ; Martinoia, Enrico ; Marten, Irene ; Hedrich, Rainer

Abstract: Proton pumping of the vacuolar-type H(+)-ATPase into the lumen of the central plant organelle generates a proton gradient of often 1-2 pH units or more. Although structural aspects of the V-type ATPase have been studied in great detail, the question of whether and how the proton pump action is controlled by the proton concentration on both sides of the membrane is not understood. Applying the patch clamp technique to isolated vacuoles from Arabidopsis mesophyll cells in the whole-vacuole mode, we studied the response of the V-ATPase to protons, voltage, and ATP. Current-voltage relationships at different luminal pH values indicated decreasing coupling ratios with acidification. A detailed study of ATP-dependent H(+)-pump currents at a variety of different pH conditions showed a complex regulation of V-ATPase activity by both cytosolic and vacuolar pH. At cytosolic pH 7.5, vacuolar pH changes had relative little effects. Yet, at cytosolic pH 5.5, a 100-fold increase in vacuolar proton concentration resulted in a 70-fold increase of the affinity for ATP binding on the cytosolic side. Changes in pH on either side of the membrane seem to be transferred by the V-ATPase to the other side. A mathematical model was developed that indicates a feedback of proton concentration on peak H(+) current amplitude (v(max)) and ATP consumption (K(m)) of the V-ATPase. It proposes that for efficient V-ATPase function dissociation of transported protons from the pump protein might become higher with increasing pH. This feature results in an optimization of H(+) pumping by the V-ATPase according to existing H(+) concentrations.

DOI: https://doi.org/10.1074/jbc.M111.310367

Luminal and cytosolic pH feedback on proton pump activity and ATP affinity of the V-type ATPase from *Arabidopsis**

Florian Rienmüller[1], Ingo Dreyer[2], Gerald Schönknecht[3], Alexander Schulz[1], Karin Schumacher[4], Réka Nagy[5], Enrico Martinoia[5], Irene Marten[1] and Rainer Hedrich[1,6]

[1]From the University of Würzburg, Institute for Molecular Plant Physiology and Biophysics, Julius-von-Sachs Platz 2, D-97082 Würzburg, Germany

[2]Centro de Biotecnologia y Genomica de Plantas, Universidad Politécnica de Madrid, Plant Biophysics, Campus de Montegancedo, Carretera M-40, km 37.7, 28223-Pozuelo de Alarcón (Madrid), Spain

[3]University of Heidelberg, Heidelberg Institute for Plant Sciences, Im Neuenheimer Feld 360, 69120 Heidelberg, Germany

[4]Oklahoma State University, Department of Botany, Stillwater, Oklahoma 74078

[5]Institute of Plant Biology, University of Zürich, Zollikerstrasse 107, Zurich, Switzerland

[6]Second affiliation: KSU King Saud University, Riyadh, Saudi Arabia

*Running title: *pH-dependent action of V-type ATPases from Arabidopsis*

To whom correspondence should be addressed: Rainer Hedrich, University of Würzburg, Institute for Molecular Plant Physiology and Biophysics, Julius-von-Sachs Platz 2, D-97082 Würzburg, Germany, Tel. +49-931-3186100, E-mail: hedrich@botanik.uni-wuerzburg.de, and Ingo Dreyer, Centro de Biotecnologia y Genomica de Plantas, Universidad Politécnica de Madrid, Plant Biophysics, Campus de Montegancedo, Carretera M-40, km 37.7, 28223-Pozuelo de Alarcón (Madrid), Spain, Tel. +34-91-336 4588, E-mail: ingo.dreyer@upm.es

Keywords: *Arabidopsis*; ATP; pH regulation; proton transport; vacuolar ATPase

Background: Vacuolar H^+-ATPases use ATP to generate a transmembrane proton motive force.
Results: Cytosolic and vacuolar pH affect proton transport rate and ATP binding of V-ATPases.
Conclusion: With decreasing pH the dissociation of transported protons from V-ATPase seems to be hindered.
Significance: V-ATPase activity is optimized according to existing H^+ concentrations via close coupling between the ATP-binding and proton-translocating complex.

SUMMARY

Proton pumping of the vacuolar-type H^+-ATPase into the lumen of the central plant organelle generates a proton gradient of often 1-2 pH units or more. Although structural aspects of the V-type ATPase have been studied in great detail, the question whether and how the proton pump action is controlled by the proton concentration and -gradient is not understood. Applying the patch clamp technique to isolated vacuoles from *Arabidopsis* mesophyll cells in the whole-vacuole mode, we studied the response of the V-ATPase to protons, voltage and ATP. Current-voltage relationships at different transmembrane pH gradients, indicated decreasing coupling ratios at increasing ΔpH. A detailed study of ATP-dependent H^+-pump currents at a variety of different pH conditions showed a complex regulation of V-ATPase activity by both cytosolic and vacuolar pH. At cytosolic pH 7.5, vacuolar pH changes had relative little effects. Yet, at cytosolic pH 5.5, a 100-fold increase in vacuolar proton concentration resulted in a 70-fold increase of the affinity for ATP binding on the cytosolic side. Changes in pH on either side of the membrane seem to be

transferred by the V-ATPase to the other side.

A mathematical model was developed that indicates a feedback of proton concentration and pH gradient on peak H^+ current amplitude (v_{max}) and ATP consumption (K_M) of the V-ATPase. It predicts that for efficient V-ATPase function dissociation of transported protons from the pump protein becomes higher with decreasing pH. This results in an optimization of H^+ pumping by the V-ATPase according to existing H^+ concentrations.

Among the F-, A- and V-type family of ATP synthases and ATPases, the best characterized member is the F_oF_1-ATP synthase (see for review 1). It consists of a F_o and a F_1 complex which differ in their physicochemical and functional properties. During interconversion between energy stored in an electrochemical proton gradient and chemical energy stored in ATP, the hydrophilic F_1 domain binds ATP, and the membrane-embedded hydrophobic F_o complex mediates translocation of protons across the membrane. ATP hydrolysis in F_1 can drive transmembrane H^+ transport in F_O against an electrochemical potential gradient, or an existing proton motive force (PMF) can be used to synthesize ATP, as in photophosphorylation and oxidative phosphorylation. For coupling proton transport to ATP synthesis/hydrolysis, the F_o and F_1 domains function as rotary motors (2), which are coupled by elastic mechanical-power transmission (3). In order to function primarily as a synthase, it was proposed that the H^+/ATP coupling ratio *c* reflecting the interconversion of the energy - stored in the electrochemical gradient - into ATP should be about 4. Thereby the consumption of more protons per ATP synthesized would assure the maintenance of a high phosphorylation potential (2). Instead, a smaller coupling value (about 2) would be preferable when the enzyme acts as an ATPase. If fewer protons were pumped per hydrolyzed ATP, a larger electrochemical gradient would be maintained (2).

During the evolution of proton-translocating F_oF_1 complexes at least two functional conversions have probably occurred with one leading first from an ancestral ATPase of an anaerobe to an ATPase in prokaryotes followed by the transformation of some ATP synthases to endomembrane/vacuolar ATPases (2,4). The latter functional transition appears to be related to a duplication and fusion of the gene encoding the c-subunit within the F_0 complex and loss of proton-binding carboxylates in amino acids of the c-subunit (2). This notion is partially supported by the fact that some ATP synthases from anaerobic Archaea e.g. *Archaeoglobus fulgidus* or *Methanothermobacter thermoautotrophicus* are characterized by double-sized c-subunits (4-6). With further bisection of the H^+/ATP coupling ratio from 4 to 2 for the change in primary function from an ATP synthase to an ATPase, the electro-enzymes optimize performance in response to the thermodynamics, given by the unique environments of the host organelle in question (e.g. chloroplasts for ATP synthases vs. vacuoles for ATPases).

During photophosphorylation the pH of the thylakoid lumen acidifies without strong polarization of the photosynthetic membrane. ATP synthases that function in photophosphorylation in chloroplasts thus predominately use the proton gradient of the PMF for ATP formation. Instead, under physiological conditions the vacuolar ATPase uses the chemical energy of ATP provided by photophosphorylation or oxidative phosphorylation to pump protons into the lumen of the central plant organelle. As a result a pH gradient - in the order of 1 to 2 pH units and more - and an electrical field across the vacuolar membrane are generated. The latter, however, is only weak (7,8) because of compensatory counter-balancing ion fluxes. The PMF provides a versatile energy store which can be used on demand to e.g. accumulate metabolites such as sugars in antiport with protons (9). Under experimental conditions, when in patch clamp studies a cytosol-directed pH gradient was established and ADP and P_i rather than ATP was present at the cytosolic side of isolated vacuoles, the V-ATPase can also work as an ATP synthase (10, cf.11,12).

Given the V-type ATPase operates as H^+ pumping ATPase under physiological conditions at luminal proton concentrations, differing from the cytosolic one by an order of magnitude or more, proper electro-enzyme function should require a feedback via changes in luminal- and cytosolic pH. Therefore, to gain insights in the pH dependency of the V-ATPase, here we performed patch-clamp experiments with isolated vacuoles from *Arabidopsis* mesophyll cells. Proton pump kinetics and current-voltage relationships were obtained from whole-vacuole recordings in the presence and absence of ATP under defined cytoplasmic and vacuolar pH.

EXPERIMENTAL PROCEDURES

Plant material and vacuole isolation. Growth conditions of *Arabidopsis thaliana* ecotype Columbia (Col-0), *det3-1*, *vha-a2 vha-a3* and *tpc1-2* mutant were as previously described (9). According to (13) mesophyll cell protoplasts were isolated for subsequent release of the vacuoles via treatment with a hypotonic solution (10 mM EGTA, 10 mM HEPES/Tris pH 7.5, osmolality of 200 mosmol kg^{-1} adjusted with D-sorbitol).

Electrophysiology. According to the convention for electrical measurements on endomembranes (14) patch clamp experiments on vacuoles were performed in the whole-vacuole configuration essentially as previously described (9,15). An EPC7 or an EPC10 patch clamp amplifier (HEKA, http://www.heka.com) was used for macroscopic current recordings from mesophyll cell vacuoles at a data acquisition rate of 2 ms (EPC7), 10 ms or 100 µs (EPC10). After macroscopic currents were low-pass filtered at 30 Hz (EPC7) or 100 Hz (EPC10), data were digitized by an ITC-16 (EPC7) (INSTRUTECH CORP., http://www.instrutech.com/) or the integral LIH8+8 of the EPC10 (HEKA, http://www.heka.com/). The data were stored on windows-environment computers. The clamped voltages were corrected for the liquid junction potential (16). Different software programs such as Pulse, Patchmaster (HEKA) and IGOR PRO (WAVE METRICS INC., http://www.wavemetrics.com) were used for data acquisition and off-line analysis. Macroscopic currents were normalized to the membrane capacitance (C_m) of the respective vacuole to allow quantitative comparison of the proton transport capacity among different vacuoles. The holding potential for V-ATPase measurements was usually set to 0 mV if not otherwise stated. Voltage ramps (1 mV/ms) were applied in a range either between -180 mV and 100 mV within 270 ms or between -250 mV to 100 mV within 340 ms.

Patch clamp solutions. Symmetrical bath and pipette solutions were used generally composed of 100 mM KCl, 5 mM $MgCl_2$ and 1 mM $CaCl_2$. The media were set to an osmolality of 400 mosmol kg^{-1} with D-sorbitol. pH values were adjusted to pH 7.5 and 6.5 with 10 mM HEPES/Tris, to pH 5.5 with 10 mM MES/Tris and to pH 9.5 with 10 mM BTP/MES. Mg-ATP (SIGMA, http://www.sigmaaldrich.com) was added from an ATP stock solution to the bath medium facing the cytosolic side of the vacuolar membrane side. Thereby the ATP-free bath solution was replaced by the ATP-containing one either upon bath perfusion in the recording chamber or via an application pipette in front of the respective vacuole (9). Variations in the composition of the solutions are given in the figure legends.

Estimation of the coupling ratio c. The coupling ratio *c* is defined as number of protons translocated per hydrolyzed ATP molecule, or free energy of ATP hydrolysis divided by free energy required to pump one proton.

$$c = \frac{\Delta G_{ATPhydrolysis}}{\Delta \mu H^+} \qquad \text{(Eq. 1)}$$

With $\Delta G_{ATP\ hydrolysis} = -30.27$ kJ mol^{-1} (17) and

$$\Delta \mu H^+ = F \cdot (\Delta \Phi - 59\ mV \cdot \Delta pH) \qquad \text{(Eq. 2)}$$

where *F* is the Faraday constant (96500 C/mol), $\Delta\Phi$ is the electric potential difference, and $\Delta pH = pH_{cyt} - pH_{vac}$, the coupling ratio *c* is calculated as

$$c = \frac{-30.27\ kJ/mol}{F \cdot (\Delta \Phi - 59\ mV \cdot (pH_{cyt} - pH_{vac}))} \qquad \text{(Eq. 3)}$$

RESULTS

ATP-powered V-ATPase currents and polarization of the vacuolar membrane. The V-type ATPase interconverts metabolic energy and electrochemical proton gradient. Although its structure and biological role becomes increasingly well understood (18 and paper cited therein), their quantitative electrochemical function and regulation is not yet fully understood. To gain insights into this issue, in our patch clamp analysis we focused on the model plant *Arabidopsis thaliana*. Following isolation of mesophyll cell protoplasts, vacuoles were liberated on demand directly in the patch clamp chamber upon selective osmotic swelling and rupture of the plasma membrane (15,19). To record ATPase-mediated currents from the entire V-type proton pump population, the whole vacuole configuration was established applying a short high-voltage pulse in the vacuole-attached mode. As a result the membrane patch under the patch pipette was broken allowing equilibration of the vacuole lumen with the pipette electrolyte solution (9). Under this condition proton currents associated with ATP hydrolysis were recorded. For this, the V-

ATPase population was activated upon ATP application to the cytoplasmic side of the vacuolar membrane via perfusion pipettes (9,19) or bath perfusion. Different experimental conditions under which competing transport processes did not take place or were largely reduced were used for recording of the ATP-induced proton currents. In order to minimize or even eliminate interfering background current components such as the SV/TPC1 channels, ATP-induced pump currents were monitored at zero membrane voltage under symmetrical ionic conditions and defined cytoplasmic and vacuolar pH. When the proton pumps of wild type vacuoles were challenged with 5 mM ATP and pH buffered to symmetrical pH 7.5 in the bath and patch pipette, outward currents of about 2.5 pA/pF were measured (Fig. 1A). In order to test whether these currents were indeed mediated by ATP-activated V-ATPases, the specific V-ATPase inhibitor bafilomycin (BF, 500 nM) was added to the bath solution as soon as the steady-state level in proton pump activity was reached. In the presence of BF the ATP-dependent currents ceased (Fig. 1A). In addition, the V-ATPase-dependent ability for membrane polarization was tested in the current clamp mode. With cytosolic pH 6.5 and luminal pH 7.5, proton pumps powered by 5 mM ATP hyperpolarized the vacuolar membrane potential by -72.4 mV in wild type and -3 mV in the V-ATPase deficient mutant *vha-a2 vha-a3* (Fig. 1B; (18)).

V-ATPase proton pumping requires VHA-a and -C subunits. V-ATPases consist of two domains with different structure and function. The peripheral ATP-hydrolyzing V_1 complex is composed of eight subunits (VHA-A to -H), whereas the integral V_0 complex contains six subunits (VHA-a, -c, -c′, -c″, -d, and -e) and is engaged with proton translocation (20). Recently, we demonstrated that the double mutant *vha-a2 vha-a3* lacks V-ATPase-mediated ATP hydrolysis and proton currents (18). To test the effect of changes in the peripheral V_1 complex on V-ATPase activity, in a similar approach we analyzed vacuoles from the *det3-1* mutant. The *DET3* gene which encodes the subunit C of the V-ATPase was shown to contain a T→A mutation in the *det3-1* mutant that very likely leads to a reduced V-ATPase activity (21). When compared to the situation in wild type (100%) and the *vha-a2 vha-a3* double mutant, pump currents in *det3-1* vacuoles evoked upon the treatment with 5 mM ATP were reduced by about 62% (Suppl. Figs. 1A & B). This result points to a tight coupling between the ATP-hydrolyzing function of V_1 complex and the proton-channel function of the integral V_0 complex.

Coupling ratio is pH-dependent. An ideal coupling ratio *c* of two protons pumped for each hydrolyzed ATP molecule was proposed for V-ATPases (2). Early studies on V-ATPases found a stoichiometry of 2 (22-24) but later reports claimed also variable coupling ratios with up to 4 protons being transferred for each ATP hydrolyzed by the vacuolar proton pump (25-28). It was also hypothesized that the coupling ratio *c* depends on the proton concentration at both sides of the tonoplast and the membrane voltage (25,29). To address this issue, we determined the proton pump activity of the V-ATPase as a function of pH and membrane voltage. In order to avoid superimposition of the ATP-evoked pump currents by voltage-dependent SV/TPC1-channel-mediated cation currents, the patch clamp experiments were conducted with vacuoles isolated from the TPC1-loss-of-function mutant *tpc1-2* (30,31). Furthermore, potassium-selective channels of the TPK1-type (32) were blocked by substituting K^+ by Cs^+ in the patch clamp solutions (33). Under defined cytoplasmic and vacuolar pH the response of an individual vacuole to voltage ramps (1 mV/ms) was recorded prior and after ATP application. An example of the macroscopic current-voltage relationships evoked by voltage ramps in the range from -150 to +100 mV in the absence and presence of 5 mM ATP at symmetrical pH 7.5 is shown in Fig. 2A. When the current-voltage (I/V) curve monitored in the absence of ATP was subtracted from that obtained with ATP, the deduced ionic currents reflect the voltage behavior of the V-ATPase (Fig. 2B). In the absence of a pH gradient across the vacuolar membrane, ATP-induced proton currents changed direction at average at -94.5 ± 14.0 mV (n = 5). After an increase in the vacuolar proton concentration by a factor of 10 (pH_{cyt} 7.5/pH_{vac} 6.5), the V-ATPase had to transport protons against a gradient. Accordingly, proton currents at zero membrane voltage dropped in average from 2.9 ± 0.3 pA/pF (n=5) to 1.9 ± 0.1 pA/pF (n=5) and the reversal potential of the pump currents shifted from -94.5 mV to -67.5 mV ± 10.6 mV (n = 5) (Fig. 2B). In line with the consequences of a 100-fold and therefore even steeper proton gradient (pH_{cyt} 7.5/pH_{vac} 5.5), proton currents at zero membrane voltage further decreased reaching only 1.1 ± 0.1 pA/pF and currents reversed in average at -49.6

± 3.9 mV (n = 3) (Fig. 2B). Based on the reversal potential and the energy of ATP hydrolysis, the H^+/ATP coupling factor *c* was calculated for the three different pH conditions. With symmetrical pH 7.5 and 5 mM ATP, the H^+/ATP coupling factor *c* was estimated to be 3.3. When the vacuolar lumen was acidified from pH 7.5 to 6.5 (c = 2.5) and 5.5 (c = 1.9), the coupling ratio *c* decreased.

V-ATPase proton transport capacity, K_m value and ATP hydrolysis are pH-dependent. The pH-dependent function of the proton pump was further quantified on the basis of steady-state proton currents. With the membrane potential clamped to zero mV and symmetrical cytosolic pH 7.5, a peak steady-state proton-current amplitude of 2.4 ± 0.1 pA/pF was registered from wild type vacuoles in the presence of 5 mM ATP (Figs. 3A & B). These pump currents only slightly changed when the luminal pH was changed from pH_{vac} 7.5 to 5.5 (1.8 ± 0.4 pA/pF) or 9.5 (2.2 ± 0.8 pA/pF) (Fig. 3B). Unlike the luminal pH, the cytosolic proton concentration in the living plant cell only varies within a small range. However, to drive the V-type ATPase to its limit, the function of the proton pump fueled by 5mM-ATP was not just studied at physiological pH 7.5 but also at a cytosolic pH of 5.5 and 9.5. A cytosolic alkaline shift from pH_{cyt} 7.5 to 9.5 (pH_{vac} 7.5) resulted in a pronounced decrease in the V-ATPase-generated proton currents from 2.4 to 0.3 ± 0.1 pA/pF (Fig. 3B). Interestingly, these pump current amplitudes were much smaller than under pH_{cyt} 7.5/ pH_{vac} 5.5, even though the direction and magnitude of the pH gradient were the same under these two pH conditions. A cytosolic acidification to pH_{cyt} 5.5 (pH_{vac} 7.5) resulted in an increase of pump currents from 2.4 to 3.2 ± 0.1 pA/pF (Fig. 3B). Finally, at pH_{cyt} 5.5 the luminal pH was altered from 7.5 to 5.5, and as a result the pump current induced by 5 mM ATP were reduced in amplitude by 56% (to 1.4 ± 0.4 pA/pF).

In the following we asked the question whether the observed changes in current amplitudes (Fig. 3) were caused by alterations in ATP affinity or maximum transport capacity of the V-ATPase. For this, we compared the following four pH conditions: symmetrical pH 7.5, symmetrical pH 5.5, physiological pH gradient (pH_{cyt} 7.5/ pH_{vac} 5.5), and inverted pH gradient (pH_{cyt}5.5/ pH_{vac}7.5). When the ATP concentration was stepwise increased up to 10 mM, peak proton-pump currents raised following a saturation-type concentration-dependence. Fitting a Michelis-Menten function to the saturation curve for symmetrical $pH_{cyt/vac}$ 7.5 revealed a maximal proton transport capacity (v_{max}) of 2.8 pA/pF and a K_M value of 0.3 mM (Fig. 4A). When the pH gradient was directed into the cytosol (pH_{cyt}7.5/ pH_{vac} 5.5), v_{max} dropped to 1.7 pA/pF while the K_M value was 0.8 mM (Fig. 4B). Upon inversion of the pH gradient (pH_{cyt} 5.5/ pH_{vac} 7.5) proton currents did not saturate with 10 mM ATP (Fig. 4C). However, fitting a saturation curve to the latter data set allowed us to calculate a v_{max} of 4.9 pA/pF and a K_M value of 2.9 mM. Finally we tested how the pump would respond to cytosolic acidification. Therefore we buffered both the vacuole lumen and bath solution to pH 5.5 and studied the ATP dependence of proton pumping. Under these extreme cytosolic conditions ($pH_{cyt/vac}$ 5.5) v_{max} was 1.3 pA/pF, comparable to v_{max} at pH_{cyt} 7.5/pH_{vac} 5.5 (1.7 pA/pF), but by a factor of 4 lower to that at pH_{cyt} 5.5/pH_{vac} 7.5. At symmetrical pH 5.5 the K_M value dropped to 0.04 mM, almost two orders of magnitude lower compared to pH_{cyt} 5.5 and pH_{vac} 7.5 (Fig. 4). Thus, in line with the 5-mM-ATP-powered proton current amplitudes (Fig. 3B), the effect of luminal acidification on v_{max} and K_M was much higher in the presence of pH_{cyt} 5.5 than pH_{cyt} 7.5. Providing the V-ATPase with high ATP-affinity pumping at pH_{vac} 5.5 might help the cell to recover from cytosolic acidification.

Modeling pump kinetics. To understand the behavior of the pump (v_{max} and K_M values) under the different conditions tested, we developed a simple mechanistic model for the pump cycle:

$$\begin{array}{ccccc} & & \text{ATP} & \rightarrow & \text{ADP+Pi} \\ & \overset{k_1}{\rightarrow} & & \overset{k_2}{\rightarrow} & \overset{k_3}{\rightarrow} \\ \text{Pump+c}[\text{H}_{\text{cyt}}] & \underset{k_1'}{\leftarrow} & \text{H}_{\text{cyt}}\text{:Pump} & \underset{k_2'}{\leftarrow} & \text{Pump:H}_{\text{vac}} \underset{k_3'}{\leftarrow} \text{Pump+c}[\text{H}_{\text{vac}}] \end{array}$$

In this cycle cytosolic protons associate with the protein (*H_{cyt}:Pump*), are then transported to the vacuolar side (*Pump:H_{vac}*) under consumption of the energy provided by ATP hydrolysis and dissociate there. In principle, this cycle can function also in the inverse direction (10). To prove that at least some of the rate constants k_1, k_1', k_2, k_2', k_3, k_3' and/or the coupling rate, c, are pH-dependent, it was initially hypothesized that they are all pH-independent to confute this hypothesis. It is shown that under this assumption the different K_M values cannot be explained with this simple model.

In the conditions tested (especially $V = 0$ mV) the direction of proton flow is strongly biased in the cytosol → vacuole direction. Therefore, we considered only the case k_2' = 0. With this simplification, the proton current can be expressed as:

$$I = \frac{v_{max}[ATP]}{K_M + [ATP]}, \text{ with}$$

$$v_{max} = const \frac{k_1[H_{cyt}]^c}{1 + \frac{k_1}{k_3}[H_{cyt}]^c + \frac{k_3'}{k_3}[H_{vac}]^c} \text{ and}$$

$$K_M = k_1' \frac{1 + \frac{k_1}{k_1'}[H_{cyt}]^c + \frac{k_3'}{k_3}[H_{vac}]^c}{1 + \frac{k_1}{k_3}[H_{cyt}]^c + \frac{k_3'}{k_3}[H_{vac}]^c}$$

Due to the limitation of the biological system to gain data points for more extreme conditions, it is not possible to reliably assign values to the free parameters of the model. However, already the qualitative interpretation of the model allowed us to deduce far reaching hypotheses as outlined in the following. We first considered the experimental K_M values and plotted them for a better overview in a 3-dimensional plot (Fig. 5), where the x- and the y-axis denote the cytosolic (pH_{cyt}) and the vaculor pH values (pH_{vac}), respectively. When starting with the physiological condition pH_{cyt} 7.5/ pH_{vac} 5.5, K_M = 0.8 mM, then a drop in the cytosolic pH to pH_{cyt} 5.5/ pH_{vac} 5.5 or an increase in the vacuolar pH to pH_{cyt} 7.5/ pH_{vac} 7.5 results in a decrease of the K_M value. Assuming pH-independent constants in the model, such a reduction in K_M upon an increase in $[H_{cyt}]$ or a decrease in $[H_{vac}]$ can only be explained if $k_1/k_3 > k_1/k_1$', *i.e.* $k_1' > k_3$ (for details see Appendix). Otherwise, the K_M would be constant ($k_1' = k_3$) or would increase ($k_1' < k_3$.) under the considered changes. However, a relation $k_1' > k_3$ would be contradictory to the observation upon a change to the condition pH_{cyt} 5.5/ pH_{vac} 7.5. It is observed that the K_M increases; but with $k_1' > k_3$ it would be predicted to decrease (see Appendix). Thus, the initial assumption that all constants are pH-independent is confuted. For the coupling rate c a pH dependency was experimentally shown. Yet, some of the rate constants are likely to be pH-dependent as well. For instance, the whole set of data could be explained qualitatively if k_1' decreases upon a drop of pH_{cyt} (and/or k_1 increases) while k_3 increases upon an increase of pH_{vac} (and/or k_3' decreases). Physiologically, the change in k_1' (k_1) and k_3 (k_3') following pH_{cyt} and pH_{vac} changes would have a reasonable meaning: The pump protein would sense the cytosolic and the vacuolar pH, e.g. by protonation of the protein. The dissociation rates of the transported protons from the pump (k_1' and k_3) would be larger if the surrounding pH is high and smaller if the surrounding pH is low.

DISCUSSION

As outlined in this study, the vacuolar proton ATPase has peculiar features. Unlike the plant plasma membrane ATPase, which strongly hyperpolarizes the membrane (34,35), the proton pumping activity of the V-ATPase does not result in a strong hyperpolarization of the vacuolar membrane (Fig. 1B, cf. 7,8). Under symmetrical pH conditions, pump currents reverted their direction at around -95 mV (Fig. 2). This value indicates that the energy from the hydrolysis of one ATP molecule is used to transport on average 3.3 protons from the cytosol to the vacuole. This coupling is larger than the 1:1 stoichiometry of plasma membrane ATPases (see for review 36) and very likely reflects the evolutionary origin of V-ATPases from an ATP synthase. A drawback of such a strong coupling, however, is that even small

electrical gradients negatively interfere with pump activity. Consequently, V-ATPases can only establish larger pH gradients if the electrical gradient generated due to the charge transport dissipates immediately either by a shunt pathway or by other transporters harvesting this energy for their own use. This dissipation might be accomplished by a cation efflux from the vacuole or by an anion influx (37 and references therein,38). So far, there are no indications that the V-ATPase itself mediates such a favorable counter-transport. However, we know that several electrogenic transporters like voltage-independent K^+ channels or the SV channel TPC1 are dominating the electrical properties of the vacuolar membrane (37). So, we propose that the V-ATPase is acting in a fine-tuned concert with these transporters.

Another astonishing observation from the voltage dependence of the V-ATPase is the apparent pH dependency of the reversal voltage pointing to a pH-dependent H^+/ATP coupling ratio of this H^+ pump. Reports on V-ATPases from *Saccharomyces cerevisiae, Beta vulgaris and Citrus limon* also claimed variable coupling rates (25,28,29). From a structural point of view, a pH-dependent, flexible coupling ratio of the vacuolar H^+ ATPase is hard to understand. The function of proton pumping has been closely related to the double-sized c subunits of the integral V_o complex of the V-ATPase containing in total six functional carboxylate. Therefore one would assume that theoretically, six protons per full rotation of the c-ring should be transported at the expense of three ATP molecules, i.e. a coupling ratio of 2 protons per hydrolyzed ATP molecule (4). Our results question this strict correlation between carboxylates and transported protons because under symmetrical pH conditions we observed a coupling ratio of c = 3.3. It might be that in addition to the highly conserved set of carboxylates other amino acid residues could contribute to proton transport. These additional binding sides might be recruited according to actual demands. If we assume the possibility, that dissociation of all bound protons from the c-ring is not mandatory for proper rotation of the pumping machinery, the observed effects could be explained. In the case of a neutral vacuolar pH all protons tend to dissociate easily from the pump and thus the proton transport rate per hydrolyzed ATP molecule would be relatively high. If we assume the original stoichiometry of an ATP synthase, the maximum value could be 4 protons per hydrolyzed ATP molecule (4). With increasing proton concentration in the vacuolar lumen, dissociation from the c-ring is less favored and the rotary machinery may slip without releasing all protons. Such a scenario would explain the reduced coupling ratio with decreasing vacuolar pH values. We have evidences for such a scenario. A minimal model of the pH dependence of K_M values (Fig. 5) predicted that increasing proton concentrations at either side reduced the dissociation rates of protons from the pump.

A further inspection of the recorded pH-dependencies indicated a possibly even more complex regulation of the V-ATPase by cytosolic and vacuolar pH. As long as the pH on the cytosolic side was kept in the physiological range, i.e. at pH 7.5, changes in vacuolar pH had relative little effects on v_{max} and K_M (Fig. 4). After acidifying the cytosolic side to pH 5.5, in contrast, changes in vacuolar pH had a tremendous effect on v_{max} and K_M (Fig. 4). These results indicate that the cytosolic pH controls whether vacuolar pH changes have much of an effect on V-ATPase function, or not. Moreover, it is unexpected that changes in vacuolar pH can have a more dramatic effect on the binding affinity of the cytosolic ATP-binding site of the V-ATPase than cytosolic pH changes have. At a vacuolar pH of either 7.5 or 5.5 a hundred-fold change in proton concentration on the cytosolic side changed the K_M values ten- or twenty-fold, respectively. Yet, at pH_{cyt} 5.5, a hundred-fold change in vacuolar pH causes a more than 70-fold change in K_M. These results indicate that pH changes on either side of the vacuolar membrane affect the entire membrane-spanning V-ATPase and are thereby transferred to the other side of the membrane. Cytosolic pH controls the effects that vacuolar pH changes have, and, the other way around, vacuolar pH changes affect the ATP-binding site, which is on the other side of the membrane about 10 nm away.

In conclusion, we here provided evidence that the prevailing proton concentration on both sides of the membrane feeds back on the function of the V-ATPase. In fact, this feedback fine-tunes the protein to act in a most efficient way. The electrogenic structure of the tonoplast guarantees that proton pumping does not result in a huge hyperpolarization as in the case of the plasma membrane. The plasma membrane ATPase uses therefore the energy of the hydrolysis of an ATP molecule to pump just one proton across the membrane. In contrast, the V-ATPase does not need to invest most energy to overcome an electric potential. Instead it can use the energy

from ATP hydrolysis to transport more protons per ATP. The feedback of the prevailing proton concentration guarantees that the ATPase is not accidentally converted by the physiological conditions into an ATP synthase. If the proton gradient is low, the pump might act at its limit and transport as many protons as possible. If the gradient, however, gets larger, the pump would face more and more the risk to act in an inverted way. A pH-dependent reduced dissociation from the c-ring would eliminate this problem. This adaptation is probably the reason why the double-sized c subunit contains only a single functional proton-translocating carboxylate. The bisection of the functional c-subunit carboxylate during evolution of V-ATPases, however, does not necessarily mean that the transport pocket for protons in total got reduced. Instead, other amino acid side chains better suited to react on the vacuolar pH in the described way might take over the proton-translocating function of the missing c-subunit carboxylates. This behavior could be comparable with a car. On plane ground a high gear can be used to accelerate the car and to keep the speed. Uphill, however, we change gears and use a smaller gear ratio.

REFERENCES

1. Okuno, D., Iino, R., and Noji, H. (2011) *J. Biochem.* **149**, 655-664
2. Cross, R. L., and Taiz, L. (1990) *FEBS Lett.* **259**, 227-229
3. Junge, W., Sielaff, H., and Engelbrecht, S. (2009) *Nature* **459**, 364-370
4. Cross, R. L., and Müller, V. (2004) *FEBS Lett.* **576**, 1-4
5. Klenk, H. P., Clayton, R. A., Tomb, J. F., White, O., Nelson, K. E., Ketchum, K. A., Dodson, R. J., Gwinn, M., Hickey, E. K., Peterson, J. D., Richardson, D. L., Kerlavage, A. R., Graham, D. E., Kyrpides, N. C., Fleischmann, R. D., Quackenbush, J., Lee, N. H., Sutton, G. G., Gill, S., Kirkness, E. F., Dougherty, B. A., McKenney, K., Adams, M. D., Loftus, B., Peterson, S., Reich, C. I., McNeil, L. K., Badger, J. H., Glodek, A., Zhou, L., Overbeek, R., Gocayne, J. D., Weidman, J. F., McDonald, L., Utterback, T., Cotton, M. D., Spriggs, T., Artiach, P., Kaine, B. P., Sykes, S. M., Sadow, P. W., D'Andrea, K. P., Bowman, C., Fujii, C., Garland, S. A., Mason, T. M., Olsen, G. J., Fraser, C. M., Smith, H. O., Woese, C. R., and Venter, J. C. (1997) *Nature* **390**, 364-370
6. Ruppert, C., Schmid, R., Hedderich, R., and Muller, V. (2001) *FEMS Microbiol. Lett.* **195**, 47-51
7. Bethmann, B., Thaler, M., Simonis, W., and Schönknecht, G. (1995) *Plant Physiol.* **109**, 1317-1326
8. Walker, D. J., Leigh, R. A., and Miller, A. J. (1996) *Proc Natl Acad Sci U S A* **93**, 10510-10514
9. Schulz, A., Beyhl, D., Marten, I., Wormit, A., Neuhaus, E., Poschet, G., Buttner, M., Schneider, S., Sauer, N., and Hedrich, R. (2011) *Plant J.* **68**, 129-136
10. Gambale, F., Kolb, H.-A., Cantu, A.M., and Hedrich, R. (1994) *Eur. Biophys. J.* **22**, 399-403
11. Yokoyama, K., Muneyuki, E., Amano, T., Mizutani, S., Yoshida, M., Ishida, M., and Ohkuma, S. (1998) *J. Biol. Chem.* **273**, 20504-20510
12. Hirata, T., Nakamura, N., Omote, H., Wada, Y., and Futai, M. (2000) *J. Biol. Chem.* **275**, 386-389
13. Beyhl, D., Hortensteiner, S., Martinoia, E., Farmer, E. E., Fromm, J., Marten, I., and Hedrich, R. (2009) *Plant J.* **58**, 715-723
14. Bertl, A., Blumwald, E., Coronado, R., Eisenberg, R., Findlay, G., Gradmann, D., Hille, B., Kohler, K., Kolb, H. A., MacRobbie, E., and et al. (1992) *Science* **258**, 873-874
15. Ivashikina, N., and Hedrich, R. (2005) *Plant J.* **41**, 606-614
16. Neher, E. (1992) *Meth. Enzymol.* **207**, 9
17. Briskin, D. P., Basu, S., and Assmann, S. M. (1995) *Plant Physiol.* **108**, 393-398
18. Krebs, M., Beyhl, D., Gorlich, E., Al-Rasheid, K. A., Marten, I., Stierhof, Y. D., Hedrich, R., and Schumacher, K. (2010) *Proc. Natl. Acad. Sci. U S A* **107**, 3251-3256
19. Schulz-Lessdorf, B., and Hedrich, R. (1995) *Planta* **197**, 655-671
20. Cipriano, D. J., Wang, Y., Bond, S., Hinton, A., Jefferies, K. C., Qi, J., and Forgac, M. (2008) *Biochim. Biophys. Acta* **1777**, 599-604
21. Schumacher, K., Vafeados, D., McCarthy, M., Sze, H., Wilkins, T., and Chory, J. (1999) *Genes Dev.* **13**, 3259-3270

22. Bennett, A. B., and Spanswick, R. M. (1984) *Plant Physiol.* **74**, 545-548
23. Guern, J., Mathieu, Y., Kurkdjian, A., Manigault, P., Manigault, J., Gillet, B., Beloeil, J. C., and Lallemand, J. Y. (1989) *Plant Physiol.* **89**, 27-36
24. Schmidt, A. L., and Briskin, D. P. (1993) *Arch. Biochem. Biophys.* **301**, 165-173
25. Davies, J. M., Hunt, I., and Sanders, D. (1994) *Proc. Natl. Acad. Sci. U S A* **91**, 8547-8551
26. Müller, M. L., Jensen, M., and Taiz, L. (1999) *J. Biol. Chem.* **274**, 10706-10716
27. Yabe, I., Horiuchi, K., Nakahara, K., Hiyama, T., Yamanaka, T., Wang, P. C., Toda, K., Hirata, A., Ohsumi, Y., Hirata, R., Anraku, Y., and Kusaka, I. (1999) *J. Biol. Chem.* **274**, 34903-34910
28. Kettner, C., Bertl, A., Obermeyer, G., Slayman, C., and Bihler, H. (2003) *Biophys. J.* **85**, 3730-3738
29. Müller, M. L., and Taiz, L. (2002) *J. Membr. Biol.* **185**, 209-220
30. Peiter, E., Maathuis, F. J., Mills, L. N., Knight, H., Pelloux, J., Hetherington, A. M., and Sanders, D. (2005) *Nature* **434**, 404-408
31. Dadacz-Narloch, B., Beyhl, D., Larisch, C., Lopez-Sanjurjo, E. J., Reski, R., Kuchitsu, K., Muller, T. D., Becker, D., Schonknecht, G., and Hedrich, R. (2011) *Plant Cell* **23**, 2696-2707
32. Voelker, C., Gomez-Porras, J. L., Becker, D., Hamamoto, S., Uozumi, N., Gambale, F., Mueller-Roeber, B., Czempinski, K., and Dreyer, I. (2010) *Plant Biol.* **12 Suppl 1**, 56-63
33. Dunkel, M., Müller, T., Hedrich, R., and Geiger, D. (2010) *FEBS Lett.* **584**, 2433-2439
34. Blatt, M. R. (1992) *J. Gen. Physiol.* **99**, 615-644
35. Lohse, G., and Hedrich, R. (1992) *Planta* **188**, 206-214
36. Briskin, D. P., and Hanson, J. B. (1992) *J. Exp. Bot.* **43**, 269-289
37. Hedrich, R., and Marten, I. (2011) *Mol. Plant* **4**, 428-441
38. Meyer, S., Scholz-Starke, J., De Angeli, A., Kovermann, P., Burla, B., Gambale, F., and Martinoia, E. (2011) *Plant J.* **67**, 247-257

FOOTNOTES

*We are grateful to the Deutsche Forschungsgemeinschaft for generous financial support of RH (FOR1061, GK1342) and IM (GK1342).

[1]From the University of Würzburg, Institute for Molecular Plant Physiology and Biophysics, Julius-von-Sachs Platz 2, D-97082 Würzburg, Germany

[2]Centro de Biotecnologia y Genomica de Plantas, Universidad Politécnica de Madrid, Plant Biophysics, Campus de Montegancedo, Carretera M-40, km 37.7, 28223-Pozuelo de Alarcón (Madrid), Spain

[3]University of Heidelberg, Heidelberg Institute for Plant Sciences, Im Neuenheimer Feld 360, 69120 Heidelberg, Germany

[4]Oklahoma State University, Department of Botany, Stillwater, Oklahoma 74078

[5]Institute of Plant Biology, University of Zürich, Zollikerstrasse 107, Zurich, Switzerland

[6]Second affiliation: KSU King Saud University, Riyadh, Saudi Arabia

[7]The abbreviations used are: BF, bafilomycin; DTT, dithiothreitol; Eq., equation; pH_{cyt}, cytosolic pH; pH_{vac}, vacuolar pH; PMF, proton motive force; V_{rev}, reversal potential.

FIGURE LEGENDS

FIGURE 1. **ATP-dependent activation of V-ATPase-mediated proton currents in mesophyll vacuoles from *Arabidopsis thaliana*.** *A.* Outward currents were evoked upon application of 5 mM ATP to the bath solution. These ATP-induced currents vanished upon the additional application of bafilomycin (BF, 500 nM) *A* indicating that they represent V-ATPase-mediated proton currents. Bars above the current trace in *A* indicate the presence of ATP ± BF during current recording. The experiments in *A* were performed under symmetrical ionic conditions at pH of 7.5. *B.* Membrane polarization of wild type (WT) and *vha-a2 vha-a3* mesophyll vacuoles. The ATP(5 mM)-induced proton pump activity resulted in an increase of the tonoplast-voltage up to -72.4 mV for WT (black

trace) and -3 mV in the double mutant (gray traces) as indicated by the downward deflection of the voltage traces. The topmost trace represents a close-up of the middle one. Current clamp experiments in *B* were performed under balanced ionic conditions of 50 mM KCl at pH_{cyt} 6.5/ pH_{vac} 7.5.

FIGURE 2. **Voltage dependence of the V-ATPase in *tpc1-2* mesophyll vacuoles.** *A.* The macroscopic current response of an individual vacuole to a voltage ramp in the range of -150 mV to +100 mV before (black) and after (gray) addition of 5 mM ATP under symmetrical pH 7.5 is shown. The intersection of both curves provided the reversal potential of the electro-enzyme. Each current-voltage curve (I(V)) represents the average of five I(V) recorded from the same vacuole. *B.* Representative voltage-dependent net H^+ pump currents determined in the presence of pH 7.5 in the cytosol and three different vacuolar pH were shown. The net pump currents were obtained by subtracting the averaged I(V) curve (shown in *A* for pH_{vac} 7.5) recorded in the absence of ATP from that in the presence of ATP. The net pump currents under symmetrical pH 7.5 presented in *B* were derived from the I(V) curves given in *A*. The ionic conditions were equivalent to *A* except that the vacuolar pH was adjusted either to pH 7.5 (light gray), pH 6.5 (black) or pH 5.5 (dark gray). The reversal potentials were $V_{rev(pHvac7.5)}$ = -94.5 ± 14.0 mV (n = 5), $V_{rev(pHvac6.5)}$ = -67.5 ± 10.6 mV (n = 5) and $V_{rev(pHvac5.5)}$ = -49.6 ± 3.9 mV (n = 3). The experiments in *A & B* were performed with symmetrical solutions containing 50 mM CsCl and without calcium.

FIGURE 3. **Representative ATP-induced wild type V-ATPase outward currents.** *A***.** Application of 5 mM ATP resulted in an increase of proton outward currents given by an upward deflection of the current baseline. Current traces were recorded at 0 mV under symmetrical pH 7.5 or pH_{cyt} 5.5/ pH_{vac} 7.5. *B.* V-ATPase outward currents in response to 5 mM ATP under different pH conditions are shown. The number of experiments was from left to right n = 3, 6, 4, 4, 3, 6. Error bars give the standard error.

FIGURE 4. **pH dependency of the V-ATPase activity at various ATP levels.** Macroscopic proton pump currents from wild type vacuoles in response to different ATP concentrations were measured and plotted against the respective ATP concentration. Solid curves represent the fit of the data points with a Michaelis-Menten function providing the parameter v_{max} and K_M. The number of experiments were n = 3-6. Error bars represent the standard error. *A.* Balanced pH values. Filled squares shows pH_{cyt} 7.5/ pH_{vac} 7.5 with v_{max}= 2.8 pA/pF and K_M = 0.3 mM. Open squares represent pH_{cyt} 5.5/ pH_{vac} 5.5 with v_{max}= 1.3 pA/pF and K_M = 0.04 mM. *B.* Cytosol-directed pH gradient. Open diamonds indicate pH 7.5_{cyt} / 5.5_{vac} with v_{max}= 1.7 pA/pF and K_M = 0.8 mM. Closed diamonds represent pH_{cyt} 9.5 / pH_{vac} 7.5 with $v_{max} \approx$ 0.3 pA/pF. *C.* Vacuolar-directed pH gradient. Open circles represent pH_{cyt} 5.5/pH_{vac} 7.5 with v_{max}= 4.9 pA/pF and K_M = 2.9 mM. Filled symbols describe pH_{cyt} 7.5 / pH_{vac} 9.5 with $v_{max} \approx$ 2 pA/pF.

FIGURE 5. **pH dependence of the K_M values for ATP of the vacuolar proton ATPase in a 3-dimensional plot.** Data (*gray dots*) were obtained from fits with the Michaelis-Menten function to the data of Fig. 4. The spherical surface was superimposed to illustrate the locations of the data points in space.

APPENDIX

Hypothesis: k_1, k_1', k_3, k_3' and c are pH-independent.

1) The K_M value drops upon a change from pH_{cyt} 7.5 / pH_{vac} 5.5 to (a) pH_{cyt} 7.5 / pH_{vac} 7.5 and to (b) pH_{cyt} 5.5 / pH_{vac} 5.5

a) $$K_M^{(7.5cyt/5.5vac)} > K_M^{(7.5cyt/7.5vac)}$$

$$\Rightarrow \quad k_1' \frac{1+\frac{k_1}{k_1'}(10^{-7.5})^c+\frac{k_3'}{k_3}(10^{-5.5})^c}{1+\frac{k_1}{k_3}(10^{-7.5})^c+\frac{k_3'}{k_3}(10^{-5.5})^c} > k_1' \frac{1+\frac{k_1}{k_1'}(10^{-7.5})^c+\frac{k_3'}{k_3}(10^{-7.5})^c}{1+\frac{k_1}{k_3}(10^{-7.5})^c+\frac{k_3'}{k_3}(10^{-7.5})^c}$$

$$\Rightarrow \quad \left[1+\frac{k_1}{k_1'}10^{-7.5\cdot c}+\frac{k_3'}{k_3}10^{-5.5\cdot c}\right]\left[1+\frac{k_1}{k_3}10^{-7.5\cdot c}+\frac{k_3'}{k_3}10^{-7.5\cdot c}\right] > \left[1+\frac{k_1}{k_1'}10^{-7.5\cdot c}+\frac{k_3'}{k_3}10^{-7.5\cdot c}\right]\left[1+\frac{k_1}{k_3}10^{-7.5\cdot c}+\frac{k_3'}{k_3}10^{-5.5\cdot c}\right]$$

$$\Rightarrow \quad \frac{k_1}{k_3}10^{-7.5\cdot c}+\frac{k_1}{k_1'}10^{-7.5\cdot c}+\frac{k_1}{k_1'}\frac{k_3'}{k_3}10^{-7.5\cdot(c+c)}+\frac{k_1}{k_3}\frac{k_3'}{k_3}10^{-c\cdot(7.5+5.5)} > \frac{k_1}{k_3}10^{-7.5\cdot c}+\frac{k_1}{k_1'}10^{-7.5\cdot c}+\frac{k_1}{k_1'}\frac{k_3'}{k_3}10^{-c\cdot(7.5+5.5)}+\frac{k_1}{k_3}\frac{k_3'}{k_3}10^{-7.5\cdot(c+c)}$$

$$\Rightarrow \quad \frac{k_1}{k_3}\frac{k_3'}{k_3}10^{-7.5\cdot c}[10^{-5.5\cdot c}-10^{-7.5\cdot c}] > \frac{k_1}{k_1'}\frac{k_3'}{k_3}10^{-7.5\cdot c}[10^{-5.5\cdot c}-10^{-7.5\cdot c}]$$

$$\Rightarrow \quad \frac{k_1}{k_3} > \frac{k_1}{k_1'}$$

$$\Rightarrow \quad k_1' > k_3$$

b) $$K_M^{(7.5cyt/5.5vac)} > K_M^{(5.5cyt/5.5vac)}$$

$$\Rightarrow \quad k_1' \frac{1+\frac{k_1}{k_1'}(10^{-7.5})^c+\frac{k_3'}{k_3}(10^{-5.5})^c}{1+\frac{k_1}{k_3}(10^{-7.5})^c+\frac{k_3'}{k_3}(10^{-5.5})^c} > k_1' \frac{1+\frac{k_1}{k_1'}(10^{-5.5})^c+\frac{k_3'}{k_3}(10^{-5.5})^c}{1+\frac{k_1}{k_3}(10^{-5.5})^c+\frac{k_3'}{k_3}(10^{-5.5})^c}$$

$$\Rightarrow \quad \frac{k_1}{k_1'}(10^{-7.5})^c+\frac{k_1}{k_3}(10^{-5.5})^c > \frac{k_1}{k_1'}(10^{-5.5})^c+\frac{k_1}{k_3}(10^{-7.5})^c$$

$$\Rightarrow \quad \frac{k_1}{k_3} > \frac{k_1}{k_1'}$$

$$\Rightarrow \quad k_1' > k_3$$

2) The K_M value increases upon a change from pH_{cyt} 7.5 / pH_{vac} 5.5, or pH_{cyt} 5.5 / pH_{vac} 5.5 or pH_{cyt} 7.5 / pH_{vac} 7.5 to pH_{cyt} 5.5 / pH_{vac} 7.5. However, if k_1' > k_3, then

i) $$k_1' \frac{1+\frac{k_1}{k_1'}(10^{-5.5})^c+\frac{k_3'}{k_3}(10^{-7.5})^c}{1+\frac{k_1}{k_3}(10^{-5.5})^c+\frac{k_3'}{k_3}(10^{-7.5})^c} < k_1' \frac{1+\frac{k_1}{k_1'}(10^{-7.5})^c+\frac{k_3'}{k_3}(10^{-7.5})^c}{1+\frac{k_1}{k_3}(10^{-7.5})^c+\frac{k_3'}{k_3}(10^{-7.5})^c}$$

$\Rightarrow$ $K_M^{(5.5cyt/7.5vac)} < K_M^{(7.5cyt/7.5vac)}$

$\Rightarrow$ contradiction to the experimental result

---

ii) $$k_1' \frac{1+\frac{k_1}{k_1'}(10^{-5.5})^c+\frac{k_3'}{k_3}(10^{-7.5})^c}{1+\frac{k_1}{k_3}(10^{-5.5})^c+\frac{k_3'}{k_3}(10^{-7.5})^c} < k_1' \frac{1+\frac{k_1}{k_1'}(10^{-5.5})^c+\frac{k_3'}{k_3}(10^{-5.5})^c}{1+\frac{k_1}{k_3}(10^{-5.5})^c+\frac{k_3'}{k_3}(10^{-5.5})^c}$$

$\Rightarrow$ $K_M^{(5.5cyt/7.5vac)} < K_M^{(5.5cyt/5.5vac)}$

$\Rightarrow$ contradiction to the experimental result

---

iii) $$k_1' \frac{1+\frac{k_1}{k_1'}(10^{-5.5})^c+\frac{k_3'}{k_3}(10^{-7.5})^c}{1+\frac{k_1}{k_3}(10^{-5.5})^c+\frac{k_3'}{k_3}(10^{-7.5})^c} < k_1' \frac{1+\frac{k_1}{k_1'}(10^{-7.5})^c+\frac{k_3'}{k_3}(10^{-5.5})^c}{1+\frac{k_1}{k_3}(10^{-7.5})^c+\frac{k_3'}{k_3}(10^{-5.5})^c}$$

$\Rightarrow$ $K_M^{(5.5cyt/7.5vac)} < K_M^{(7.5cyt/5.5vac)}$

$\Rightarrow$ contradiction to the experimental result

Conclusion: The hypothesis is wrong. Thus, at least one of the constants k_1, k_1', k_3, k_3' and/or c must be pH-dependent. For c there is experimental evidence for such a dependency, but also the others might additionally be pH-dependent. For instance, k_1' may decrease upon a drop of pH_{cyt} (and/or k_1 increases) while k_3 increases upon an increase of pH_{vac} (and/or k_3' decreases).

FIGURE 1.

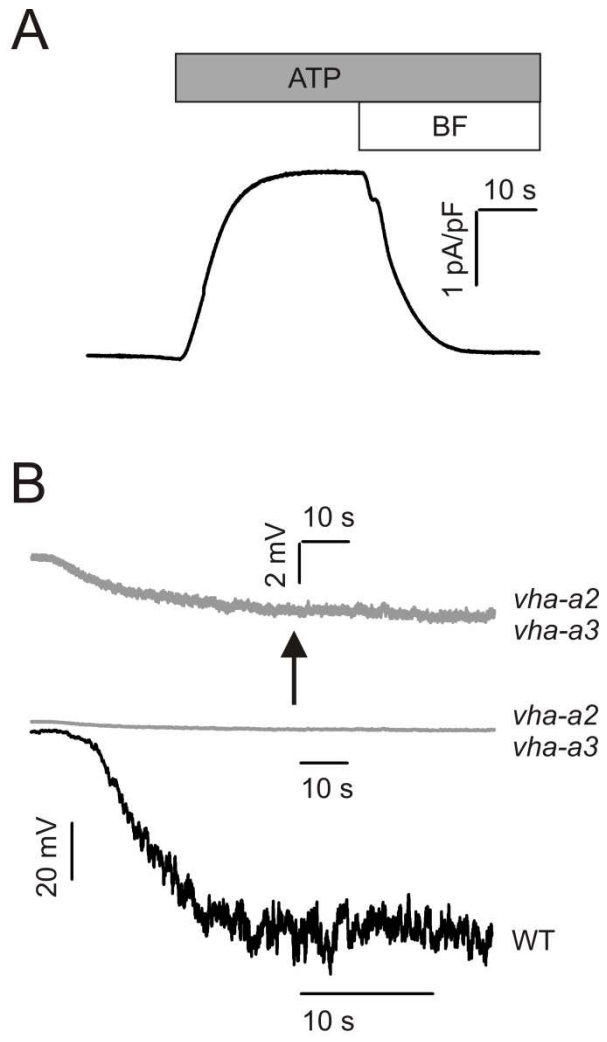
A
ATP
BF
10 s
1 pA/pF
B
10 s
2 mV
vha-a2
vha-a3
vha-a2
vha-a3
10 s
20 mV
WT
10 s

FIGURE 2.

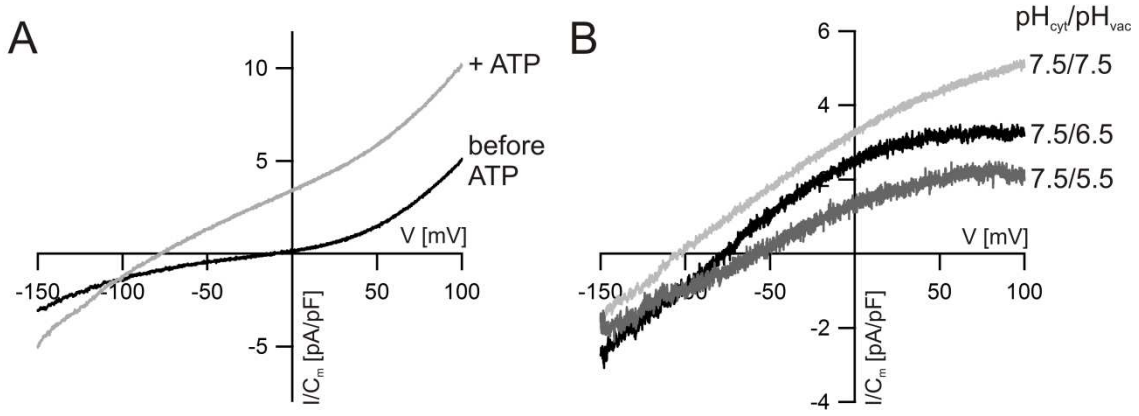
A
10
5
-5
+ ATP
before
ATP
V [mV]
-150
-100
-50
50
100
I/C$_m$ [pA/pF]
B
pH$_{cyt}$/pH$_{vac}$
6
4
-2
-4
7.5/7.5
7.5/6.5
7.5/5.5
V [mV]
-150
-50
50
100
I/C$_m$ [pA/pF]

FIGURE 3.

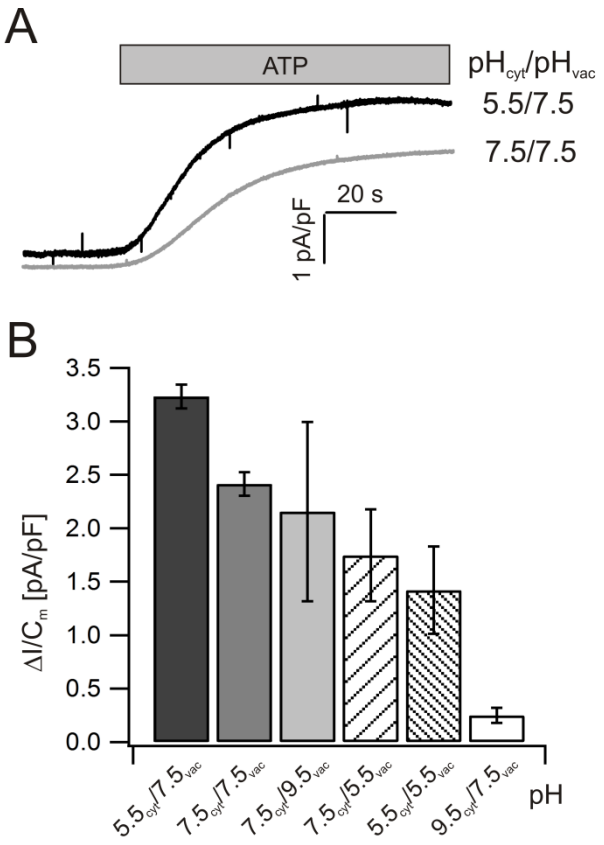
A
ATP
pH$_{cyt}$/pH$_{vac}$
5.5/7.5
7.5/7.5
20 s
1 pA/pF
B
ΔI/C$_m$ [pA/pF]
3.5
3.0
2.5
2.0
1.5
1.0
0.5
0.0
5.5$_{cyt}$/7.5$_{vac}$
7.5$_{cyt}$/7.5$_{vac}$
7.5$_{cyt}$/9.5$_{vac}$
7.5$_{cyt}$/5.5$_{vac}$
5.5$_{cyt}$/5.5$_{vac}$
9.5$_{cyt}$/7.5$_{vac}$
pH

FIGURE 4.

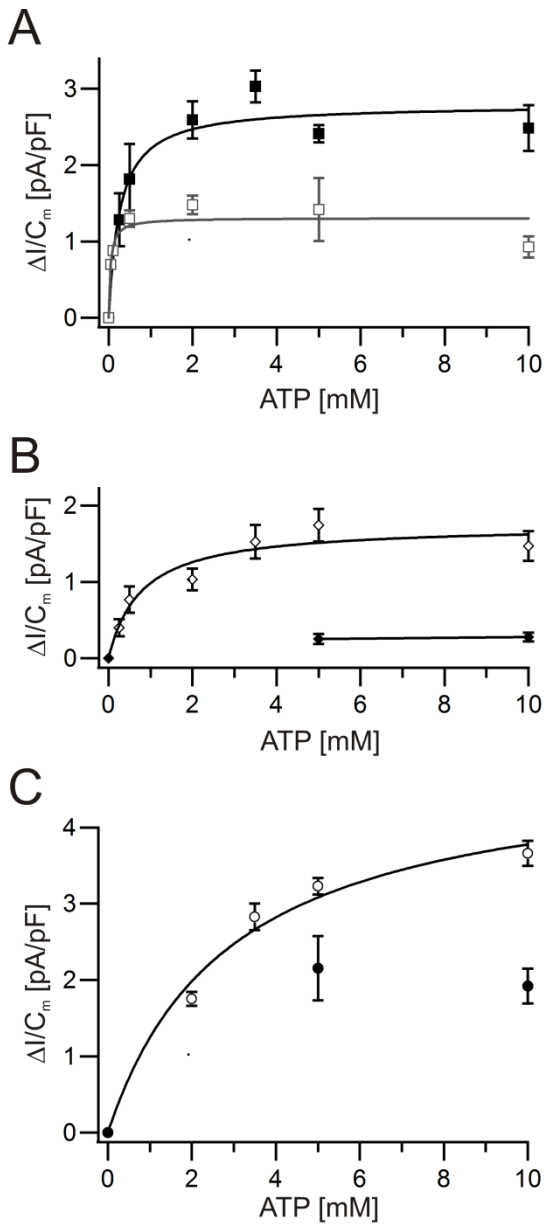

FIGURE 5.

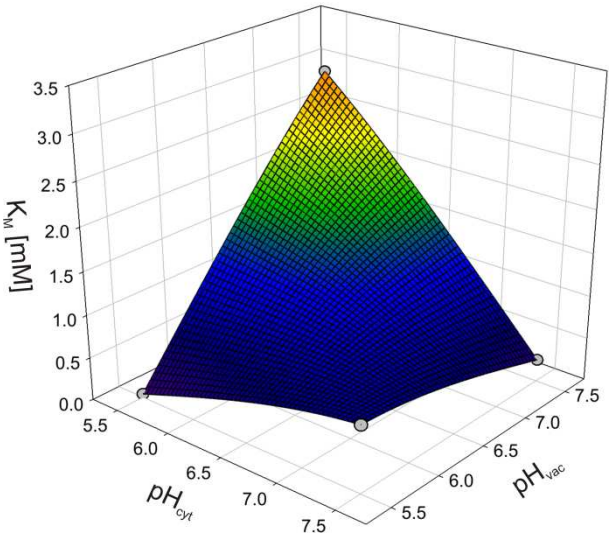
3.5
3.0
2.5
2.0
1.5
1.0
0.5
0.0
K_M [mM]
5.5
6.0
6.5
7.0
7.5
pH_{cyt}
5.5
6.0
6.5
7.0
7.5
pH_{vac}